MERLIN-DEFICIENT iPSCs AS AN *IN VITRO* MODEL SYSTEM FOR STUDIYNG *NF2* PATHOGENESIS

Núria Catasús[1], Miguel Torres-Martin[1,2], Inma Rosas[1,2], Bernd Kuebler[3], Gemma Casals-Sendra[1], Helena Mazuelas[4], Alex Negro[1,2], Francesc Roca-Ribas[5], Emilio Amilibia[5], Begoña Aran[3], Anna Veiga[3], Ángel Raya[3], Bernat Gel[4], Ignacio Blanco[1,2], Eduard Serra[4], Meritxell Carrió[4*] and Elisabeth Castellanos[1,2*]

*Equally contributed

1) Clinical Genomics Research Group, Germans Trias i Pujol Research Institute (IGTP); Can Ruti Campus, Badalona, Barcelona, Spain
2) Genetics Department, Germans Trias i Pujol University Hospital (HUGTiP), Can Ruti Campus, Badalona, Barcelona, Spain
3) Medicine Regenerative Program, Institut d'Investigació Biomèdica de Bellvitge. IDIBELL, Hospital Duran i Reynals, Gran Via de L'Hospitalet, 199-203, 08908, L'Hospitalet de Llobregat, Barcelona, Spain.
4) Hereditary Cancer Group, Germans Trias i Pujol Research Institute (IGTP); Can Ruti Campus, Badalona, Barcelona, Spain
5) Otorhinolaryngology Department, Germans Trias i Pujol University Hospital (HUGTiP), Can Ruti Campus, Badalona, Barcelona, Spain

Corresponding authors:

Meritxell Carrió (mcarriol@igtp.cat) and Elisabeth Castellanos (ecastellanos@igtp.cat/ecastellanosp.germanstrias@gencat.cat)

ABSTRACT

NF2-related schwannomatosis is an autosomal dominant syndrome that predisposes to the development of benign tumors of the nervous system. Schwannomas, particularly bilateral vestibular schwannomas (VS), are the most characteristic features of the disease. These tumors are caused by the bi-allelic inactivation of the *NF2* gene in a cell of the Schwann cell lineage. Our current understanding of the molecular pathogenesis of the *NF2* gene, as well as the development of new effective therapies is hampered by the absence of human non-perishable cell-based bearing distinct *NF2* pathogenic variants. With this aim, we generated and characterized three isogenic paired induced pluripotent stem cell (iPSC) lines with single or bi-allelic inactivation of *NF2* by combining the direct reprogramming of VS cells with the use of CRISPR/Cas9 editing. Our results show a critical function of *NF2* for the maintenance of a stable pluripotent state. However, we were able to nudge them towards the Neural Crest-Schwann Cell (NC-SC) axis by applying a 3D Schwann cell differentiation protocol. *NF2*(+/-) and *NF2*(-/-) spheroids homogeneously expressed classical markers of the NC-SC lineage. In addition, *NF2*(-/-) SC-like spheroids showed dysregulation of multiple signaling pathways already described for merlin-deficient SC, and altered in human schwannomas. Therefore, *NF2*(+/-) and *NF2*(-/-) SC-like spheroids can represent a bona fide human *in vitro* cellular model to study the role of *NF2* pathogenesis.

KEYWORDS: NF2-related schwannomatosis; Induced Pluripotent Stem Cells; Schwann Cell; Neural Crest Stem Cell; Vestibular Schwannomas, Schwannomas

55 **INTRODUCTION**

56 NF2-related schwannomatosis (NF2-related SWN; OMIM 101000) is a dominantly inherited
57 autosomal syndrome characterized by the development of multiple tumors of the nervous
58 system (1,2). The incidence of the disease is estimated to be 1 in 28,000 live births with
59 complete penetrance by the age of 60, with 50-60% of cases due to *de novo* mutations (3). The
60 pathognomonic feature of the disease is the development of bilateral vestibular schwannomas
61 (VS), well-circumscribed tumors that arise from Schwann cells (SC) in the vestibulocochlear
62 nerve, due to the bi-allelic inactivation of *NF2*. VS are responsible for hearing loss, deafness
63 and tinnitus(4). Affected individuals may also develop multiple schwannomas in other cranial,
64 spinal and peripheral nerves as well as intracranial and intraspinal meningiomas, and spinal
65 ependymomas (5–8). Cutaneous and ocular manifestations are also common (9,10). Due to
66 their number and anatomical location, these tumors, although histologically benign, are
67 responsible for high morbidity and reduced life expectancy (11). The gold standard treatment
68 for NF2 patients includes surveillance, surgery, radiotherapy and bevacizumab for VS (4),
69 although this last is associated with toxicity if used for extended periods (12), so there is an
70 important need to develop new treatments.

71 NF2-related SWN is caused by pathogenic variants in the *NF2* tumor suppressor gene
72 (22q12.2), which encodes for merlin (moesin-ezrin-radixin-like) protein, a scaffold protein that
73 interacts with transmembrane receptors and intracellular effectors to mediate mitogenic,
74 survival, proliferation and cell-cell contact signaling pathways (13–15). Changes in merlin result
75 in the inhibition of cell proliferation and the dysregulation of a wide variety of signaling
76 cascades from the cell surface to the nucleus. One of the most studied roles of merlin is its
77 involvement in the Hippo signaling pathway, by repressing YAP/TAZ nuclear translocation.
78 Once in the nucleus, YAP and TAZ associate with the DNA-binding TEAD proteins (TEADs 1-4) to
79 activate the expression of regulators of the cell cycle and apoptosis (16). Merlin also controls
80 cell proliferation by contact inhibition through mechanisms that include the formation of

81 stable adherens junctions, and the regulation of specific growth factor receptors, the focal
82 adhesion kinase (FAK) and phosphoinositide 3-kinase (PI3K)/AKT/mTOR pathways (16). In
83 addition, merlin is known to be involved in other signaling pathways such as the
84 Ras/Raf/MAPK, TP53 and the Rac1-Pak1 pathways (17,18).
85 Studying the pathogenesis of the *NF2* gene and developing potential therapies remains
86 challenging due to the lack of durable preclinical models that recapitulate the genetics and
87 pathophysiology of NF2-realted tumors. Initial attempts to generate *in vivo* mouse models
88 revealed the essential role of *NF2* during embryogenesis and early development (19). In
89 *NF2*(+/-) mutant mice, the absence of a single *NF2* allele causes the appearance of malignant
90 epithelial tumors and sarcomas with an aggressive tendency to metastasize (20). Conditional
91 KO murine models can generate schwannomas and VS (21–23). In addition, several patient-
92 derived xenograft (PDX) mouse models have also been developed, with varied levels of success
93 in recapitulating the biology of human NF2-related SWN traits (24). In addition, *in vitro*,
94 primary SC cultures derived from VS have been set up (25,26), although the limited lifespan of
95 primary cultures can severely constrain their use for extended experiments. Transformed and
96 immortalized VS-derived cell lines have been developed to overcome this limitation and have
97 been widely used as platforms for drug screening (HEI-93, JEI-001) (27,28), although these
98 models undergo physiological changes due to the immortalization process, severely reducing
99 the value of any comparison with primary cells.
100 Induced pluripotent stem cell (iPSC) (29) models have been used in a wide range of diseases
101 and represent an unlimited source of cells with multiple applications such as disease
102 modelling, drug development, regenerative medicine, or gene regulation (30–33). The first
103 NF2-related SWN model reported was an iPSC line harboring a homozygous variant in the *NF2*
104 gene (UMi031-A-2), obtained by CRISPR/Cas9 gene-editing of an unaffected pluripotent cell
105 line (34); and, more recently, an iPSC clone was derived from mononuclear bone marrow stem
106 cells from a mosaic NF2-related SWN patient (35).

107 One of the main defining characteristics of iPSCs is their ability to differentiate into the three
108 germ layers, and thus their potential to differentiate into any cell type involved in NF2-related
109 SWN traits. Protocols have been developed to differentiate iPSC towards the SC lineage,
110 passing through an intermediate multipotent neural crest stage (36–38). Using these
111 protocols, it has been shown that iPSC-derived SCs show homogeneous expression of SC
112 markers and the ability to myelinate axons when co-cultured with dorsal root ganglia neurons
113 (38). Therefore, the use of iPSCs appears to be a suitable human cellular model to study the
114 molecular pathogenesis of the *NF2* gene, and the differentiation capacity and growth behavior
115 of the *NF2* deficient SC-derived cells that originate NF2-related schwannomas.
116 In the present study, we generated three isogenic iPSC lines harboring single or bi-allelic loss-
117 of-function variants in the *NF2* gene by direct reprogramming of VS cells and the use of
118 CRISPR/Cas9 editing. For the first time, these cells were characterized and differentiated
119 towards the NC-SC lineage, resulting in *NF2*(+/-) and *NF2*(-/-) SC-like spheroids co-expressing
120 classic markers of the NC-SC axis. In addition, *NF2*(-/-) SC-like spheroids showed dysregulation
121 of several signaling pathways previously described in *NF2*(-/-) cells, providing a bona fide *in*
122 *vitro* cellular model to study the role of *NF2* pathogenesis.
123

124 **MATERIALS AND METHODS**

125 All procedures performed were in accordance with the ethical standards of the IGTP Human
126 Research Ethics Committee (CEIC) (PI-17-250), which approved this study, and with the 1964
127 Helsinki declaration and its later amendments. The "*Comisión de Garantías para la Donación y*
128 *Utilización de Células y Tejidos Humanos, ISCIII*") authorized the Project.
129 **Patients and Vestibular Schwannoma samples:** tumor samples were obtained from NF2-
130 related SWN patients clinically managed at the Spanish Reference Centre (CSUR) for
131 phacomatoses HUGTiP-ICO-IGTP, diagnosed according to standard diagnostic criteria

132 (**Supplemental Table S1**) (39). Written informed consent was obtained for iPSC generation and
133 genomic analysis. Tumor samples were processed as described in Castellanos et al., 2018 (40).
134 **Reprogramming of Vestibular Schwannomas:** between $0.2 \cdot 10^6$-$1 \cdot 10^6$ of VS derived cells were
135 reprogrammed using the CytoTune™-iPS 2.0 Sendai Reprogramming Kit (Thermo Fisher
136 Scientific), a non-integrative cell reprogramming method holding the four Yamanaka factors
137 (OCT4, SOX2, KLF4, and cMYC), according to manufacturer's instructions.
138 **Tumor and iPSC molecular characterization:** genetic analysis was performed using the
139 customized I2HCP panel as previously described (41) or Whole Exome Sequencing (WES). The
140 latter was performed using KAPA HyperCap technology with KAPA HyperExome Probes (Roche)
141 according to manufacturer's instructions and sequenced in a NextSeq instrument (Illumina).
142 Analysis of small nucleotide variants was performed with Mutect2 and annotated with
143 Funcotator (42). Potential SNV and small indels were detected among the original cell lines and
144 the paired CRISPR lines, GATK 4.2.6.1 was used for the entire process (42) (**Supplemental**
145 **Material and Methods**). To detect *NF2* splicing variants, tumors were studied both at RNA and
146 DNA level. *NF2* variants were confirmed by Sanger Sequencing. SNP-array analysis was
147 assessed using Illumina HumanOmniExpress v1 BeadChips (730,525 SNPs) according to
148 manufacturers' instructions and as described in Supplemental Material and Methods.
149 **CRISPR/Cas9 gene edition in iPSC lines:** CRISPR/Cas9 editing was performed with the ArciTect
150 ribonucleoprotein (RNP) system (STEMCELL Technologies). The designed sgRNA targeted exon
151 2 of the *NF2* gene (GTACACAATCAAGGACACAG) using the Synthego - CRISPR Design Tools
152 (https://www.synthego.com/products/bioinformatics/crispr-design-tool). TransIT-X2®
153 Dynamic Delivery System (Mirus) was used for transfection according to manufacturers'
154 instructions.
155 **iPSC culture:** iPSCs were grown on growth factor-reduced Matrigel (BD Biosciences)-coated 6-
156 well plates and cultured in mTESR Plus medium (STEMCELL Technologies). iPSCs were split
157 using Accutase (Merk) and cells were seeded with Rock Inhibitor (STEMCELL Technologies)

158 (1:1000) for 24h. When required, visibly differentiated cells were removed manually from the
159 culture of *NF2*(-/-) cells. In this study, the *NF2*(+/+) FiPS line (FiPS Ctrl 1-SV4F-7) was used for all
160 experiments as a control.

161 **Neural Crest (NC) differentiation:** differentiation of iPSC lines into NC was performed as
162 previously described in Menendez et al. (2013) (37) with minor modifications (38). $9x10^4$ iPSCs
163 were seeded on matrigel-coated dishes in mTESR Plus medium. The following day, the medium
164 was replaced with Neural Crest Differentiation Media (**Supplemental Material and Methods**)
165 and was replaced every day. NC were maintained in this medium and split with Accutase when
166 necessary.

167 **Differentiation into SC in 2D:** to establish SC differentiation, $0.4x10^6$ NC cells/well were plated
168 onto 0.1mg/mL poly-L-lysine (Sigma) and 4µg/mL laminin (Gibco) 6-well plates and cultured in
169 SC differentiation media (SCDM) (**Supplemental Material and Methods**) as previously
170 described (38).

171 **Differentiation towards SC in 3D:** NC cells were detached with Accutase and, $2.25{\cdot}10^6$
172 cells/well were seeded onto AggreWell TM800 24-well plates (Stem Cell Technologies) in 2mL
173 SCDM (described above). The medium was changed twice a week removing 1 mL and replacing
174 1 mL of fresh SCDM. On days 7, 14 and 30 spheroids were collected and processed for
175 subsequent analysis.

176 **Flow cytometry:** accutase-dissociated cells were resuspended in PBS-0.1% BSA and incubated
177 with p75 primary antibody and subsequently incubated with Alexa Fluor 568 secondary
178 antibody, followed by the incubation of Hnk1 primary antibody that was detected with Alexa
179 Fluor 488-conjugated secondary antibody. Antibodies were incubated 30 min on ice. Flow
180 cytometry analysis was performed using BD LSR Fortessa SORP and BD FACS Diva 6.2 software.

181 **Immunocytochemistry:** cells or spheroids were fixed in 4% paraformaldehyde in PBS for 15min
182 at room temperature (RT), permeabilized with 0.1%Triton-X 100 in PBS for 10 min at RT,
183 blocked in 10% FBS in PBS for 15 min at RT, and incubated with the indicated antibodies

184 (**Supplemental Table M1**) overnight at 4°C. Secondary antibodies Alexa Fluor 488 and Alexa
185 Fluor 568 were incubated for 1h at RT. Nuclei were stained with DAPI and images captured
186 using LEICA DMIL6000 and LASAF software.

187 **RNA processing, sequencing and analysis:** Total RNA extraction from iPSCs, NC cells and SC-
188 differentiating spheroids was extracted with the 16 LEV simplyRNA Purification kit (Promega),
189 following manufacturer's instructions. RNA was quantified with a Nanodrop 1000
190 spectrophotometer (Thermo Scientific). The polyA RNA libraries were sequenced on an
191 Illumina Novaseq 6000 in 150 bp pair-end mode. For RNAseq processing, genome GRCh37.p13
192 and gene annotation gencode version 19 were used. Reads were aligned with STAR version
193 2.7.10a (43) and count files were produced with QoRTs version 1.3.6 (44). These raw counts
194 were used for DESeq2 differential expression (DE) analysis with Wald significance test and
195 Benjamini & Hochberg correction (FDR) correction. A corrected p-value of 0.01 and an absolute
196 Log2-fold change of 1 was used for considering a gene as DE. Volcano plots were performed
197 using EnhancedVolcano (with the https://github.com/kevinblighe/EnhancedVolcano) outputs
198 from Deseq2. To account for more direct measurement, barplots in Figure 2 were instead
199 normalized by Trimmed Mean of M-values from EdgeR (45) and then RPKMs were calculated
200 for every gene. The *vst* normalization from DESeq2 (46) was used for unsupervised cluster
201 heatmaps with Euclidean metric and Ward method. PCA features were chosen using the top
202 2000 genes with the highest SD over vst normalization. Pathway enrichment analyses for DE
203 genes were performed using GSEA pre-ranked test (47) using the "stat" value from Deseq2. A
204 FDR <0.05 was considered as significant. Single sample GSEA (ssGSEA) with MSigDB version
205 2022.1.Hs (48) was used when comparing more than two groups of samples. Enrichr (49,50)
206 was used only with DE genes as input. The 41 raw fastq files schwannomas for comparison
207 were retrieved from the EGA repository with accession code EGAD00001002722, and were
208 processed with the same methodology described above. For re-analysis of this cohort together
209 with our set, vst values were recalculated for all of them without correction for batch.

210

211 **RESULTS**

212 1. Generation of IPSC harboring single or bi-allelic pathogenic variants in the *NF2* gene

213 Three VS from three independent NF2-related SWN patients that met standard diagnostic
214 criteria (39) were used for reprogramming (VS-25, VS-245 and VS-267) with the aim of
215 obtaining iPSC clones harboring pathogenic variants present in NF2 patients. Molecular
216 characterization of these tumors through the I2HCP panel (41) and SNP-array analysis
217 uncovered the *NF2* alterations reported in **Supplemental Table S1** and **Supplemental Figure**
218 **S1**. Except for the alteration in the *NF2* locus, no pathogenic variants were identified in any
219 known oncogene or tumor suppressor gene. The non-integrating Sendai virus vector (SeV)
220 encoding the 4 Yamanaka factors (29) was used to induce pluripotency of VS-dissociated cells
221 and we determined the *NF2* genotype of the generated single-cell clones through Sanger
222 sequencing (**Figure 1A, Supplemental Table S2**).

223 From VS-25 and VS-267, only clones carrying the germline *NF2* pathogenic variant (*NF2*(+/-))
224 were obtained. One clone derived from each tumor was selected for further characterization.
225 From VS-245, a VS coming from a mosaic patient, we obtained both *NF2*(-/-) and *NF2*(+/+) iPSC
226 clones, named VSi-245. As VSi-245(+/+) clones were reprogrammed from an unaffected cell,
227 these were not further characterized. In contrast, all nine VSi-245 *NF2*(-/-) iPSC clones analysed
228 sustained the exogenous expression of Yamanaka factors by the Sendai (SeV) construct for
229 more than 40 passages after reprogramming and, therefore, were also discarded for the rest
230 of the study (**Supplemental Figure S2**).

231 With the aim of achieving iPSCs with complete *NF2* inactivation, and given the low efficiencies
232 obtained in the generation of *NF2*(-/-) clones by VS reprogramming, we used the CRISPR/Cas9
233 technology to edit the *NF2* gene in both, the *NF2*(+/-) VSi-25 and VSi-267 iPSCs and a control
234 *NF2*(+/+) iPSC line (FiPS Ctrl 1-SV4F-7, registered in the Spanish National Stem Cell Bank/
235 ESiO44C in https://hpscreg.eu/)). Thus, using CRISPR/Cas9 RNP complexes, we targeted exon 2

236 of the *NF2* gene and obtained single-cell *NF2*(-/-) iPSC clones from VS-derived lines (named 25-
237 CasD7, when derived from VSi-25, and 267-CasD2 when derived from VSi-267) and isogenic
238 *NF2*(+/-) and *NF2*(-/-) iPSC clones derived from the control line (named FiPS-CasB2 and FiPS-
239 CasH6, respectively). Pathogenic variants in *NF2* were fully characterized through PCR and
240 Sanger sequencing and the *NF2* coding region was cloned to confirm compound heterozygous
241 clones (**Table 1**). In addition, all *NF2* genotypes were confirmed through a merlin western blot
242 (**Figure 1B**). From this point on, we worked on the characterization of three pairs of isogenic
243 iPSC lines: three with one truncating variant in *NF2* and three lines carrying the bi-allelic
244 inactivation of *NF2* (two pairs VS-reprogrammed and one from a control iPSC line (**Table 1**)).
245
246 iPSCs: induced pluripotent stem cell; VS: vestibular schwannoma; FiPS; fibroblasts induced pluripotent
247 stem cell; Ctrl: Control; WT: wild-type
248
249 1.1. Characterization of *NF2* (+/-) and *NF2* (-/-) iPSC
250 All clones analysed expressed cell surface proteins and transcription factors associated with
251 pluripotency: Oct4, SSEA-3, SSEA-4, Nanog, Sox2, Tra-1-60 and Tra-1-81; were positive for
252 alkaline phosphatase staining; and showed karyotype stability after at least 20 passages (46,
253 XY) (**Supplemental Figure S3, A-C**). Although all iPSC clones expressed the typical pluripotent
254 markers, we could observe differences in clone morphology between *NF2*(+/-) and *NF2*(-/-) cell
255 lines. Whereas *NF2*(+/-) showed classical iPSC colony morphology, edited *NF2*(-/-) iPSCs
256 presented less compact colony formation, eventually aggregating in the center of the colony,
257 growing upwards and undergoing major spontaneous differentiation compared with the iPSC
258 control line (**Figure 1C**). Furthermore, *NF2*(+/-) iPSCs showed the capacity to differentiate into
259 the three primary germ layers *in vitro* (mesoderm, endoderm, and ectoderm) through
260 embryoid bodies (EBs) formation. In contrast, *NF2*(-/-) lines could not be differentiated using

261 standard EBs generation protocols and required direct differentiation to acquire expression of
262 the three germ layers (**Figure 1D, Supplemental Table S3**).
263 Genomic characterization of *NF2*(+/-) VSi-25 and VSi-267 iPSCs selected clones by SNP-array
264 analysis and WES showed no differences with respect to the tumor of origin, with the
265 exception of the absence of the the second hit in the *NF2*(+/-) lines (**Supplemental Figure S1**).
266 Generated *NF2*(-/-) iPSC lines revealed no pathogenic off-target alterations by WES analysis of
267 the edited lines (**Supplemental Table S4**).
268 We have therefore generated three *NF2* iPSCs isogenic pair lines (*NF2*(+/-) and *NF2*(-/-)) with
269 three different genomic backgrounds and cells of origin, providing an unlimited source of cells,
270 consisting of a biological triplicate system. The phenotype observed in all three *NF2*(-/-) lines,
271 which showed relevant phenotypic and differentiation abnormalities, suggests that the *NF2*
272 gene may play a role in maintaining a purely pluripotent state.
273

274 **2. *NF2* iPSC differentiation towards the NC-SC lineage**

275 Given that the cells that initiate schwannoma formation in NF2-related SWN are *NF2*(-/-) cells
276 derived from the SC lineage, we applied a differentiation protocol towards the NC-SC axis. As a
277 first step, we generated NC by applying a chemically defined differentiation protocol as
278 previously reported (37). After ten days of NC differentiation, cells achieved NC morphology
279 (**Figure 2A**). Cell identity was assessed by flow cytometry of NC markers, NGFR (Nerve Growth
280 Factor Receptor) (p75) and HNK1 (CD57), at early passages of the NC differentiation process
281 (p4) and in a mature NC state (p8). *NF2(+/+)* an *NF2(+/-)* cells showed high expression of both
282 markers already at p4 which increased up to more than 80% at a mature NC state. *NF2*(-/-)
283 cells already showed some expression of p75 and Hnk1 at the iPSC stage which increased at
284 p4, but did not acquire the same percentages of p75 and Hnk1-positive cells at the mature NC
285 stage (65-80%), compared with their controls *NF2(+/+)* and *NF2(+/-)* counterparts (**Figure 2B**).

286 Immunocytochemistry and transcriptome analysis (RNA-seq) of NC derived cells showed that
287 all lines expressed NC markers Sox10, TFAP2A and p75 and showed no expression of
288 pluripotency markers POU5F1 (Oct4), Nanog and Sox2 (**Figure 2C and 2D**). However, some *NF2*
289 *(-/-)* NC cells were also expressing S100B at both the RNA and protein levels, which was
290 consistent with the heterogeneity detected by flow cytometry assays. Nonetheless, although
291 *NF2*-deficient lines exhibited a distinct phenotype, they could be differentiated towards a NC-
292 like identity, were able to maintain self-renewal capacity for at least 18 passages and could be
293 cultured after several freeze-thaw cycles.
294 A last step in the differentiation towards SC, consisted of inducing the differentiation of the
295 established NC cultures into a SC state. Thus, NC cells were cultured in SC differentiation
296 medium (SCDM) for 30 days, as previously described (37,38). However, five days after inducing
297 SC differentiation, *NF2*(+/-) and *NF2*(-/-) cells showed difficulties in maintaining adherence to
298 culture dishes, in contrast to the control line, which after seven days of differentiation already
299 showed a more elongated spindle morphology resembling SC-like cells (**Supplemental Figure**
300 **S4**). We reasoned that the poor adherence capacity observed compromised their ability to
301 differentiate towards a SC identity in the standard 2D stablished conditions, and therefore, we
302 tested their capacity to differentiate in 3D conditions, following a previously established
303 protocol (51) with minor modifications.
304
305 2.1 NC-SC lineage marker analysis on *NF2*(+/-) and *NF2*(-/-) spheroids
306 To evaluate the SC differentiation capacity of *NF2*(+/-) and *NF2*(-/-) cell lines in 3D, we studied
307 the transcriptome at three time points (7, 14 and 30 days) of the differentiation process.
308 Principal component analysis (PCA) revealed that iPSCs, NCs and SCs triplicates clustered
309 according to cell type, regardless of genotype or differentiation state (**Figure 3A**).
310 At the RNA level, we observed that *NF2*(+/+) differentiating spheroids expressed typical SC
311 lineage markers (S100B, MPZ or PLP1) already at day 7. At day 14 of differentiation, *NF2*(+/+)

312 spheroids were positive for p75 and S100B markers identified by immunostaining (**Figure 3B**)
313 and expressed SC markers closely resembling those expected in SCs (**Supplemental Figure S5**).
314 However, at day 30 of differentiation the expression of some SC markers decreased (SOX10,
315 PLP1) whereas some central nervous glial markers appeared (FABP7, ASTN1), suggesting loss of
316 SC commitment. For this reason, we decided to analyse samples at day 14 of differentiation
317 (**Supplemental Figure S5**). *NF2*(+/-) VSi-25 and VSi-267 cell lines formed spheroids that stained
318 positive for p75 and S100B markers, as did the three *NF2*(-/-) cell lines (**Figure 3B**). However,
319 we were unable to obtain spheroids from the FiPS-CasB2 *NF2*(+/-) edited cell line despite
320 several attempts (**Supplemental Figure S6**).
321 RNAseq analysis revealed that *NF2*(+/-) and *NF2*(-/-) cell lines expressed high levels of SC
322 markers such as CDH19, GAP43, MPZ, PLP1 or S100B at 14 days of differentiation, in a similar
323 way to the *NF2*(+/+) control line, indicating that NC cells were progressing from a precursor
324 state into a committed SC phenotype (**Figure 3C**). Finally, we used a recently published *in vitro*
325 NC-SC expression roadmap (50) to analyze the *NF2*(-/-) cell lines (51) and they displayed a very
326 similar NC-SC expression roadmap to that previously determined for *NF2*(+/+) differentiating
327 SCs in 2D (**Supplemental Figure S7**) (51). Overall, we successfully obtained *NF2*(+/-) and *NF2*(-/-
328) SC-like spheroids, that express NC-SC lineage markers at the RNA and protein levels, by
329 applying 3D SC differentiation conditions in three isogenic paired lines.
330

331 **3. Merlin-related pathway analysis in the *NF2*(-/-) SC-like cells**

332 To better characterize *NF2*(-/-) SC-like spheroids and the effect of the absence of *NF2* on them,
333 we performed differential expression analysis of the distinct genotypes at 14 days of SC
334 differentiation stage. Only 125 genes were differentially expressed (DEG) when comparing
335 *NF2*(+/+) and *NF2*(+/-) genotypes; most of them related to cellular polarity, cell adhesion and
336 to the mTOR-pI2K-Akt signalling pathway; and some of them directly regulated by merlin, such
337 as CHL1 (52) (**Supplemental Figure S8A-B**). A higher number of DEG were found when

338 comparing the *NF2*(+/+) and *NF2*(-/-) (**Supplemental Figure S8C**), as well as when comparing
339 *NF2*(+/-) and *NF2*(-/-) (2874 and 3447 respectively) (**Figure 4A**), indicating that the second hit
340 in *NF2* is the driver of the major expression changes in these cells.
341 As it was not possible to obtain *NF2*(+/+) lines from SWN-related NF2 patients, we focused on
342 comparing *NF2*(+/-) and *NF2*(-/-) SC-like spheroids and further investigated DEG by functional
343 enrichment analyses. These showed significantly enriched Hallmark signaling pathways in
344 *NF2*(-/-) SC-like spheroids, including mTORC1, NFKβ, p53, Hedgehog, and IL6-JAK-STAT3,
345 among others, most of them directly or indirectly regulated by merlin. Other altered signaling
346 pathways were Epithelial Mesenchymal Transition (EMT), cholesterol homeostasis and fatty
347 acids metabolism, ROS signaling, hypoxia and apoptosis, Wnt/β-cantenin and finally (α and γ)
348 interferon response (**Figure 4B**). Similar results were obtained when comparing *NF2*(+/+) vs the
349 *NF2*(-/-) SC-like spheroids (**Supplemental Figure S8D**).
350 Further analyses were performed using single sample gene set enrichment analysis (ssGSEA) to
351 test whether signaling pathways previously described in merlin-deficient cells were
352 systematically altered in all *NF2(-/-)* SC-like spheroids. First, we examined the levels of TAZ
353 target genes since their expression is negatively regulated by merlin. As expected from merlin
354 deficiency, TAZ target genes were upregulated in *NF2*(-/-) SC-like spheroids. Similar results
355 were observed for TEAD2 target genes, although we observed variability between cell lines
356 (**Figure 4C**). Expression levels of genes regulated by the focal adhesion kinase (FAK) and
357 phosphoinositide 3-kinase (PI3K)/AKT/mTOR pathways, activated in the absence of merlin,
358 were upregulated in all three *NF2*(-/-) SC-like spheroid lines. (**Figure 4C**).
359 We also examined the expression of specific genes known to be altered in both *NF2*(-/-)
360 primary SCs and schwannomas and compared their normalized expression levels between the
361 three genotypes. Alterations were found in laminin receptor α6 integrin (Itga6), α-dystroglycan
362 (Dag1), and collagen (Col1a2), consistent with an alteration of basal cytoskeletal organization
363 in *NF2*(-/-) SC-like spheroids when comparted to *NF2*(+/+) and *NF2*(+/-) spheroids (**Figure 4D**).

364 In addition, analysing the status of the Hippo pathway signaling, we were able to confirm that
365 some of the major YAP target genes described in SC, involved in cell growth, proliferation and
366 migration, were significantly up-regulated in SC-like spheroids lacking *NF2* (*CCND1, CYR61,*
367 *ANKRD1, AXL*) (**Figure 4D**).
368 Altogether, these findings showed that the alterations and differentiation properties of *NF2*(-/-
369) iPSC-derived SC-like spheroids could be attributed to the lack of merlin. Moreover, these
370 results highlight a strong correlation between the previously described altered signaling
371 pathways and gene expression profile in merlin-deficient SC and that observed in *NF2*(-/-) iPSC-
372 derived SC-like spheroids at 14 days of differentiation, indicating that these cells could
373 represent a genuine *in vitro* human NF2 SC model system.
374 GSEA analysis comparing *NF2*(+/-) and *NF2*(-/-) SC-like cells revealed that other relevant merlin
375 targets previously found to be altered in schwannomas were also upregulated in the *NF2*(-/-)
376 spheroids, such as the previously mentioned MEK, PI3K-AKT/mTOR, TP53, TNFα-NFκB
377 signaling, or *ERBB2* signaling pathways, inflammatory response as well as the EMT (**Figure 4B**).
378 We confirmed this by specifically interrogating expression levels of *MAPK1*, *KRAS*, *AKT*, *TP53*,
379 *NFKB* and *VEGFA* (**Supplemental Figure S9A**). These analyses indicated that *NF2*(-/-) SC-like
380 cells could recapitulate profile signatures observed in NF2-related schwannomas.
381 To further explore this hypothesis, we compared the transcriptome of these cells at 14 days of
382 differentiation with published transcriptomes of 41 schwannomas (EGAD00001002722) (53).
383 PCA revealed that the second component was driven by the *NF2* genotype (**Supplemental**
384 **Figure S9B**), thus, we extracted the top 500 genes with higher weight for each feature, and
385 selected sub-clusters where schwannomas and *NF2*(-/-) SC-like cells showed a similar pattern
386 of expression compared to cells harboring at least one copy of *NF2* (**Figure 5A**). EnrichR
387 pathway analysis of these 500 genes showed 160 (out of 273) of them were upregulated in
388 *NF2*(+/-) and *NF2*(+/+) SC-like cells and were enriched in cell motility and extracellular
389 organization, therefore related to merlin's function (**Figure 5B**). On the other hand, 113 genes

390 in merlin deficient schwannomas and SC-like cells were enriched in axonogenesis and
391 neurogenesis (**Supplemental Figure S9C**). These results suggest that schwannomas and *NF2*(-/-
392) SC-like spheroids share a common pattern of gene expression for key pathways related to
393 *NF2* biology compared to wild type cells.
394 Overall, we successfully applied 3D SC differentiation conditions to *NF2*(+/-) and *NF2*(-/-) to
395 obtain spheroids expressing NC-SC lineage markers at RNA and protein level (**Figure 5C**). In
396 addition, gene expression of iPSC-derived merlin-deficient differentiating SCs showed that
397 these cells constitute a bona fide cellular model for the study of the *NF2* role in Schwann cells,
398 and potentially in any cell type associated with *NF2* pathogenesis.
399
400 **DISCUSSION**
401 In this work we show the generation of an unperishable human iPSC-based model for the
402 study of the molecular pathogenesis of the *NF2* gene. We have differentiated the generated
403 isogenic iPSCs towards the NC-SC lineage and shown that *NF2*(-/-) SC-like spheroids share gene
404 expression patterns with *NF2*(-/-) cells and schwannomas.
405 We first aimed to generate *NF2*(-/-) iPSCs from VS reprogramming to obtain cell lines that
406 recapitulate the genetic background of a VS constituent cell. Our results showed low
407 efficiencies in reprogramming NF2-deficient VS cells and we were not able to generate *NF2*(-/-)
408 iPSCs through this process, hypothesizing that *NF2* could have a relevant role in achieving
409 pluripotency due to its essential role in embryogenesis and early stages of development (19),
410 which is also consistent with the reported essential function of *NF2* in haploid human iPSCs
411 and leukemia cells (54,55). Reprogramming resulted in the generation of two *NF2*(+/-) lines
412 (VSi-25 and VSi-267), and their *NF2* deficient isogenic cell lines (25-CasD7, 267-CasD2) were
413 obtained by CRIPR/Cas editing. A third isogenic paired iPSC line was obtained by editing the
414 control FiPS iPSC line (*NF2*(+/-) FiPS_CasB2 and *NF2*(-/-) FiPS-CasH6). Thus, in this study we
415 generated a triplicate of paired *NF2*(+/-) and *NF2*(-/-) iPSC lines by combining direct

416 reprogramming of VS cells and *NF2* gene editing, as has been recently reported (34). In our
417 hands, the three *NF2*(-/-) iPSC lines required extensive experimental care, showed aberrant
418 colony morphology and were susceptible to spontaneous differentiation. No differences were
419 observed between the three lines, hinting that observed phenotypes are due to the lack of
420 merlin and not to the iPS cell of origin. All these factors taken together point to an essential
421 role for *NF2* in the maintenance of pluripotency of diploid cells. The three isogenic paired iPSC
422 lines generated in this study represent a valuable and non-perishable source of cells with
423 single or bi-allelic inactivation of *NF2*, which could be used as a NF2-cell based model to
424 develop further assays and to study the role of *NF2* in human cells (56).
425 Here, we showed that both *NF2*(+/-) and *NF2*(-/-) iPSCs have the capacity to differentiate into a
426 NC identity, although *NF2*(-/-) NC cultures exhibited an unstable NC phenotype, with some
427 cells undergoing spontaneous differentiation and expression of S100B and requiring a higher
428 confluence in culture to maintain their NC identity, consistent with the role of merlin in
429 cytoskeleton maintenance and control of proliferation by cell-cell contact inhibition (57–59).
430 Also, in line with these findings, in the process of differentiation of NCs into SCs, we observed
431 that both *NF2*(+/-) and *NF2*(-/-) cells were easily detached from the cell culture surface,
432 eventually leading to cell death and preventing the generation of SC-like cultures. However,
433 and most importantly, we overcame this limitation by successfully generating *NF2*(+/-) and
434 *NF2*(-/-) spheroids growing in suspension, as had been previously reported for other SC-based
435 spheroids (51). These spheroids expressed classical NC-SC markers after seven days in SCDM
436 and preserved a previously characterized *in vitro* NC-SC differentiation expression roadmap as
437 control iPSCs (51). Therefore, for the first time, we have achieved merlin-deficient SC-like cells.
438 *NF2*(-/-) SC-like spheroids showed deregulation of several signaling pathways as previously
439 described in *NF2*(-/-) SC. As expected for merlin deficiency the Hippo pathway was
440 downregulated and YAP/TAZ targets were overexpressed (*Cyr61, AXl1, ANKRD1, CCND1*) (60),
441 while mTORC1 signaling was upregulated (61), as previously described in schwannomas,

442 meningiomas and arachnoidal merlin- deficient cells, (60), consistent with the hypothesis that
443 deregulation of mTORC1 activation, in addition to the Hippo pathway, underlies the aberrant
444 growth and proliferation of NF2-deficient cells (62). Differentiated *NF2*(-/-) SC-like cells also
445 showed upregulation of well-known merlin-related cytoskeletal organization markers, such as
446 Itga6, Dag1 and Col1a2 (63). Furthermore, *NF2*(-/-) SC-like cells overexpressed inflammatory
447 response, ROS and NFkB-related pathways, most probably by Rac1 deregulation as described
448 in NF2-tumor models and merlin-deficient cells (53,64–67). Finally, merlin-deficient SC-like
449 cells also showed upregulation of TP53, VEGF and epithelial-to-mesenchymal transition
450 signaling, which is known to be deregulated in schwannomas (17,53,68–72). These results
451 confirmed the strong correlation between the described and observed changes in signaling
452 pathways and gene expression due to merlin deficiency, suggesting that the cells developed in
453 this study could be a reliable *in vitro* human NF2 SC model system to study the molecular
454 pathogenesis of *NF2*. In addition, because there are expression patterns described in
455 schwannomas that reproduce in merlin-deficient SC-like spheroids; if they were validated *in*
456 *vivo*, these cells would be an *in vitro* cellular model for schwannoma cells, which could be used
457 as a platform for drug screening.
458
459 **CONCLUSION**
460 In this study, we generated three isogenic paired *NF2*(+/-) and *NF2*(-/-) iPSC lines through
461 reprogramming VS and *NF2* editing. According to our results, the *NF2* gene seems to play a
462 relevant role in the maintenance of pluripotency. For the first time, iPSCs with different *NF2*
463 genotypes were differentiated into NC-SC lineage cells, although *merlin*-deficient iPSCs
464 exhibited an altered differentiation capacity. The application of a 3D SC differentiation
465 protocol resulted in the successful generation of *NF2*(+/-) and *NF2*(-/-) SC-like spheroids
466 expressing NC-SC lineage markers. In addition, *NF2*(-/-) SC-like spheroids showed dysregulation
467 of several signaling pathways previously described in merlin-deficient Schwann cells, such as

mTOR and Hippo-YAP, amongst others. Therefore, *NF2*(-/-) SC-like spheroids constitute a valuable resource for studying *NF2* biology in Schwann cells and potentially in any cell type associated with *NF2* pathogenesis.

CONFLICT OF INTEREST STATEMENT

The authors declare no competing interests

ACKNOWLEDGEMENTS

We thank the HGTP Clinical Services and staff for their collaboration in generating and collecting patient samples. We thank the IGTP Flow Cytometry and IGTP Genomics core facilities and their staff for their contribution and technical support. We would like to acknowledge the constant support of the different NF lay associations: *Asociación de Afectados de Neurofibromatosis*, Chromo22 and ACNefi. This study has been funded by the Chromo22 Patients association; the *Instituto de Salud Carlos III* through the project PI20/00215 (Co-funded by European Regional Development Fund "A way to make Europe"), and through the project AC22/00033, partner of the EJP RD. The EJP RD initiative has received funding from the European Union's Horizon 2020 research and innovation program under grant agreement N°825575"; funded also by *Fundació La Marató de TV3* (126/C/2020), the Children's Tumor Foundation (CTF-2019-05-005, CTF-2022-05-005), Fundación Proyecto Neurofibromatosis, the Catalan NF Association (AcNeFi), and the Government of Catalonia (SGR-Cat 2021 - 00967).

AUTHOR CONTRIBUTIONS

492 **NC**: Collection and/or assembly of data; Data analysis and interpretation; Manuscript writing;
493 **MT-M, BG:** Data analysis and interpretation; **AN, BK, IR, GC-S, BA:** Collection and/or assembly
494 of data; **HM, AV, AR, IB:** Scientific input; **FR-R, EA**: Provision of study material or patients; **ES,**
495 **MC, EC:** Conception and design; Financial support; Manuscript writing; Final approval of
496 manuscript.

497

498 **DATA AVAILABILITY STATEMENT**

499 The authors confirm that the data supporting the findings of this study are available within the
500 article [and/or] its supplementary materials. Raw data for WES and RNAseq is allocated at the
501 European Geno-Phenome Archive (EGA) with accession number (XXXXXXXXX) and will be made
502 available to external researchers upon reasonable requests.

503

504

505 **REFERENCES**

506 1. Evans DGR, Moran A, King A, Saeed S, Gurusinghe N, Ramsden R. Incidence of vestibular
507 schwannoma and neurofibromatosis 2 in the North West of England over a 10-year
508 period: Higher incidence than previously thought. Otology and Neurotology.
509 2005;26(1):93–7.

510 2. Plotkin SR, Messiaen L, Legius E, Pancza P, Avery RA, Blakeley JO, et al. Updated
511 diagnostic criteria and nomenclature for neurofibromatosis type 2 and
512 schwannomatosis: An international consensus recommendation. Genetics in Medicine.
513 2022;24(9):1967–77.

514 3. Evans DG, Bowers NL, Tobi S, Hartley C, Wallace AJ, King AT, et al. Schwannomatosis: A
515 genetic and epidemiological study. J Neurol Neurosurg Psychiatry. 2018 Jun 14;

516 4. Lloyd SKW, Evans DGR. Neurofibromatosis type 2 (NF2): diagnosis and management.
517 1st ed. Vol. 115, Handbook of clinical neurology. Elsevier B.V.; 2013. 957–67 p.

518 5. Evans DGR, Huson SM, Donnai D, Neary W, Blair V, Newton V, et al. A genetic study of
519 type 2 neurofibromatosis in the United Kingdom . II . Guidelines for genetic counselling.
520 1992;(3):847–52.

521 6. Parry DM, Eldridge R, Kaiser-Kupfer MI, Bouzas EA, Pikus A, Patronas N.
522 Neurofibromatosis 2 (NF2): Clinical characteristics of 63 affected individuals and clinical
523 evidence for heterogeneity. Am J Med Genet. 1994;52(4):450–61.

524 7. Baser ME, Makariou E V., Parry DM. Predictors of vestibular schwannoma growth in
525 patients with neurofibromatosis Type 2. J Neurosurg. 2002 Feb;96(2):217–22.

526 8. Forde C, King AT, Rutherford SA, Hammerbeck-Ward C, Lloyd SK, Freeman SR, et al.
527 Disease course of neurofibromatosis type 2: A 30-year follow-up study of 353 patients
528 seen at a single institution. Neuro Oncol. 2021 Jul 1;23(7):1113–24.

529 9. Ragge NK, Baser ME, Klein J, Nechiporuk A, Sainz J, Pulst SM, et al. Ocular abnormalities
530 in neurofibromatosis 2. Am J Ophthalmol [Internet]. 1995;120(5):634–41. Available
531 from: http://dx.doi.org/10.1016/S0002-9394(14)72210-X

532 10. Plana-Pla A, Bielsa-Marsol I, Carrato-Moñino C. Diagnostic and Prognostic Relevance of
533 the Cutaneous Manifestations of Neurofibromatosis Type 2. Actas Dermosifiliogr. 2017
534 Sep 1;108(7):630–6.

535 11. Hexter A, Jones A, Joe H, Heap L, Smith MJ, Wallace AJ, et al. Clinical and molecular
536 predictors of mortality in neurofibromatosis 2: A UK national analysis of 1192 patients. J
537 Med Genet. 2015 Aug 14;52(10):699–705.

538 12. Plotkin SR, Duda DG, Muzikansky A, Allen J, Blakeley J, Rosser T, et al. Multicenter,
539 prospective, phase II and biomarker study of high-dose bevacizumab as induction
540 therapy in patients with neurofibromatosis type 2 and progressive vestibular
541 schwannoma. Journal of Clinical Oncology. 2019;37(35):3446–54.

542 13. McClatchey AI, Giovannini M. Membrane organization and tumorigenesis - The NF2
543 tumor suppressor, Merlin. Genes Dev. 2005;19(19):2265–77.

544 14. Gladden AB, Hebert AM, Schneeberger EE, McClatchey AI. The NF2 Tumor Suppressor,
545 Merlin, Regulates Epidermal Development through the Establishment of a Junctional
546 Polarity Complex. Dev Cell [Internet]. 2010;19(5):727–39. Available from:
547 http://dx.doi.org/10.1016/j.devcel.2010.10.008

548 15. Petrilli AM, Merlin V, Nf I, Merlin I, Nf O. Role of Merlin / NF2 inactivation in tumor
549 biology. 2016;(December 2014):537–48.

550 16. Petrilli AM, Fernández-Valle C. Role of Merlin/NF2 inactivation in tumor biology.
551 Oncogene. 2015 Feb;35(February):537–48.

552 17. Chen H, Xue L, Huang H, Wang H, Zhang X, Zhu W, et al. Synergistic effect of Nutlin-3
553 combined with MG-132 on schwannoma cells through restoration of merlin and p53
554 tumour suppressors. EBioMedicine. 2018 Oct 1;36:252–65.

555 18. Zhou L, Hanemann CO. Merlin, a multi-suppressor from cell membrane to the nucleus.
556 Vol. 586, FEBS Letters. 2012. p. 1403–8.

557 19. McClatchey AI, Saotome I, Ramesh V, Gusella JF, Jacks T. The Nf2 tumor suppressor
558 gene product is essential for extraembryonic development immediately prior to
559 gastrulation. Genes Dev. 1997;11(10):1253–65.

560 20. McClatchey AI, Saotome I, Mercer K, Crowley D, Gusella JF, Bronson RT, et al. Mice
561 heterozygous for a mutation at the Nf2 tumor suppressor locus develop a range of
562 highly metastatic tumors. Genes Dev. 1998;12(8):1121–33.

563 21. Schulz A, Büttner R, Hagel C, Baader SL, Kluwe L, Salamon J, et al. The importance of
564 nerve microenvironment for schwannoma development. Acta Neuropathol. 2016 Aug
565 1;132(2):289–307.

566 22. Stemmer-Rachamimov AO, Louis DN, Nielsen GP, Antonescu CR, Borowsky AD, Bronson
567 RT, et al. Comparative pathology of nerve sheath tumors in mouse models and humans.
568 Cancer Res. 2004;64(10):3718–24.

569 23. Giovannini M, Robanus-Maandag E, Van Der Valk M, Niwa-Kawakita M, Abramowski V,
570 Goutebroze L, et al. Conditional biallelic Nf2 mutation in the mouse promotes
571 manifestations of human neurofibromatosis type 2 [Internet]. 2000. Available from:
572 www.genesdev.org

573 24. Ren Y, Chari DA, Vasilijic S, Welling DB, Stankovic KM. New developments in
574 neurofibromatosis type 2 and vestibular schwannoma. Neurooncol Adv. 2021;3(1):1–
575 13.

576 25. Dilwali S, Patel PB, Roberts DS, Basinsky GM, Harris GJ, Emerick KS, et al. Primary
577 culture of human Schwann and schwannoma cells: Improved and simplified protocol.
578 Hear Res. 2014;315:25–33.

579 26. Rosenbaum C, Kluwe L, Mautner VF, Friedrich RE, Mü HW, Hanemann CO. Isolation and
580 Characterization of Schwann Cells from Neurofibromatosis Type 2 Patients. 1998.

581 27. Xue L, He W, Wang Z, Chen H, Wang Z, Wu H. Characterization of a newly established
582 schwannoma cell line from a sporadic vestibular schwannoma patient [Internet]. Vol.
583 13, Am J Transl Res. 2021. Available from: www.ajtr.org

584 28. Hung G, Rhim JS, Slattery W, Lim D. Establishment and characterization of a
585 schwannoma cell line from a patient with neurofibromatosis 2. Vol. 20, INTERNATIONAL
586 JOURNAL OF ONCOLOGY. 2002.

587 29. Takahashi K, Yamanaka S. Induction of Pluripotent Stem Cells from Mouse Embryonic
588 and Adult Fibroblast Cultures by Defined Factors. 2006;2:663–76.

589 30. Shi Y, Inoue H, Wu JC, Yamanaka S. Induced pluripotent stem cell technology: A decade
590 of progress. Nat Rev Drug Discov [Internet]. 2017;16(2):115–30. Available from:
591 http://dx.doi.org/10.1038/nrd.2016.245

592 31. Papapetrou EP. Patient-derived induced pluripotent stem cells in cancer research and
593 precision oncology. Vol. 22, Nature Medicine. Nature Publishing Group; 2016. p. 1392–
594 401.

595 32. Raya Á, Rodríguez-Piz I, Guenechea G, Vassena R, Navarro S, Barrero MJ, et al. Disease-
596 corrected haematopoietic progenitors from Fanconi anaemia induced pluripotent stem
597 cells. Nature. 2009;460(7251):53–9.

598 33. Mungenast AE, Siegert S, Tsai LH. Modeling Alzheimer's disease with human induced
599 pluripotent stem (iPS) cells. Molecular and Cellular Neuroscience [Internet].
600 2016;73:13–31. Available from: http://dx.doi.org/10.1016/j.mcn.2015.11.010

601 34. Nourbakhsh A, Gosstola NC, Fernandez-valle C, Dykxhoorn DM. Characterization of
602 UMi031-A-2 inducible pluripotent stem cell line with a neurofibromatosis type 2-
603 associated mutation. Stem Cell Res [Internet]. 2021;55(June):102474. Available from:
604 https://doi.org/10.1016/j.scr.2021.102474

605 35. Ishi Y, Era T, Yuzawa S, Okamoto M, Sawaya R, Motegi H, et al. Analysis of induced
606 pluripotent stem cell clones derived from a patient with mosaic neurofibromatosis
607 type 2. Vol. 188, American journal of medical genetics. Part A. United States; 2022. p.
608 1863–7.

609 36. Jessen KR, Mirsky R. The origin and development of glial cells in peripheral nerves. Nat
610 Rev Neurosci. 2005;6(9):671–82.

611 37. Menendez L, Kulik MJ, Page AT, Park SS, Lauderdale JD, Cunningham ML, et al. Directed
612 differentiation of human pluripotent cells to neural crest stem cells. Nat Protoc. 2013
613 Jan;8(1):203–12.

614 38. Carrió M, Mazuelas H, Richaud-Patin Y, Gel B, Terribas E, Rosas I, et al. Reprogramming
615 Captures the Genetic and Tumorigenic Properties of Neurofibromatosis Type 1
616 Plexiform Neurofibromas. Stem Cell Reports. 2019;12.

617 39. Baser ME, Friedman JM, Wallace AJ, Ramsden RT, Joe H, Evans DGR. Evaluation of
618 clinical diagnostic criteria for neurofibromatosis 2. Neurology. 2002 Dec;59(11):1759–
619 65.

620 40. Castellanos E, Plana A, Carrato C, Carri M, Rosas I, Amilibia E, et al. Early genetic
621 diagnosis of neurofibromatosis type 2 from skin plaque plexiform schwannomas in
622 childhood. JAMA Dermatol. 2018 Mar 1;154(3):341–6.

623 41. Castellanos E, Gel B, Rosas I, Tornero E, Santín S, Pluvinet R, et al. A comprehensive
624 custom panel design for routine hereditary cancer testing: Preserving control,
625 improving diagnostics and revealing a complex variation landscape. Sci Rep. 2017;7.

626 42. Van der Auwera GA, O'Connor BD. Genomics in the Cloud: Using Docker, GATK, and
627 WDL in Terra [Internet]. O'Reilly Media; 2020. Available from:
628 https://books.google.es/books?id=vsXaDwAAQBAJ

629 43. Dobin A, Davis CA, Schlesinger F, Drenkow J, Zaleski C, Jha S, et al. STAR: ultrafast
630 universal RNA-seq aligner. Bioinformatics. 2013 Jan;29(1):15–21.

631 44. Hartley SW, Mullikin JC. QoRTs: a comprehensive toolset for quality control and data
632 processing of RNA-Seq experiments. BMC Bioinformatics. 2015 Jul;16(1):224.

633 45. Robinson MD, McCarthy DJ, Smyth GK. edgeR: a Bioconductor package for differential
634 expression analysis of digital gene expression data. Bioinformatics. 2010 Jan;26(1):139–
635 40.

636 46. Love MI, Huber W, Anders S. Moderated estimation of fold change and dispersion for
637 RNA-seq data with DESeq2. Genome Biol. 2014;15(12):550.

638 47. Subramanian A, Tamayo P, Mootha VK, Mukherjee S, Ebert BL, Gillette MA, et al. Gene
639 set enrichment analysis: A knowledge-based approach for interpreting genome-wide
640 expression profiles [Internet]. 2005. Available from:
641 www.pnas.orgcgidoi10.1073pnas.0506580102

642 48. Barbie DA, Tamayo P, Boehm JS, Kim SY, Moody SE, Dunn IF, et al. Systematic RNA
643 interference reveals that oncogenic KRAS-driven cancers require TBK1. Nature. 2009
644 Nov 5;462(7269):108–12.

645 49. Kuleshov M V., Jones MR, Rouillard AD, Fernandez NF, Duan Q, Wang Z, et al. Enrichr: a
646 comprehensive gene set enrichment analysis web server 2016 update. Nucleic Acids
647 Res. 2016 Jul 8;44(1):W90–7.

648 50. Prakash YS, Singh A, Shannon CP, Kim YW, Demarco ML, Gauvreau GM, et al. Identifying
649 Molecular Mechanisms of the Late-Phase Asthmatic Response by Integrating Cellular,
650 Gene, and Metabolite Levels in Blood Mucins and Their Sugars Critical Mediators of
651 Hyperreactivity and Inflammation [Internet]. Vol. 13, Ann Am Thorac Soc. 2016.
652 Available from: www.atsjournals.org.www.atsjournals.org.

653 51. Mazuelas H, Magallón-Lorenz M, Fernández-Rodríguez J, Uriarte-Arrazola I, Richaud-
654 Patin Y, Terribas E, et al. Modeling iPSC-derived human neurofibroma-like tumors in
655 mice uncovers the heterogeneity of Schwann cells within plexiform neurofibromas. Cell
656 Rep [Internet]. 2022 Feb;38(7):110385. Available from:
657 https://linkinghub.elsevier.com/retrieve/pii/S2211124722001061

658 52. Chen J, Jiang C, Fu L, Zhu CL, Xiang YQ, Jiang LX, et al. CHL1 suppresses tumor growth
659 and metastasis in nasopharyngeal carcinoma by repressing PI3K/AKT signaling pathway
660 via interaction with integrin β1 and merlin. Int J Biol Sci. 2019;15(9):1802–15.

661 53. Agnihotri S, Jalali S, Wilson MR, Danesh A, Li M, Klironomos G, et al. The genomic
662 landscape of schwannoma. Nat Genet. 2016 Nov 1;48(11):1339–48.

663 54. Yilmaz A, Peretz M, Aharony A, Sagi I, Benvenisty N. Defining essential genes for human
664 pluripotent stem cells by CRISPR-Cas9 screening in haploid cells. Nat Cell Biol [Internet].
665 2018;20(5):610–9. Available from: http://dx.doi.org/10.1038/s41556-018-0088-1

666 55. Blomen VA, Májek P, Jae LT, Bigenzahn JW, Nieuwenhuis J, Staring J, et al. Gene
667 essentiality and synthetic lethality in haploid human cells. Science (1979).
668 2015;350(6264):1092–6.

669 56. Rowe RG, Daley GQ. Induced pluripotent stem cells in disease modelling and drug
670 discovery. Vol. 20, Nature Reviews Genetics. Nature Publishing Group; 2019. p. 377–88.

671 57. Curto M, McClatchey AI. Nf2/Merlin: A coordinator of receptor signalling and
672 intercellular contact. Br J Cancer. 2008;98(2):256–62.

673 58. Curto M, Cole BK, Lallemand D, Liu CH, McClatchey AI. Contact-dependent inhibition of
674 EGFR signaling by Nf2/Merlin. Journal of Cell Biology. 2007 Jun 4;177(5):893–903.

675 59. Catasús N, Rosas I, Bonache S, Negro A, Torres-Martin M, Plana-Pla A, et al. Antisense
676 oligonucleotides targeting exon 11 are able to partially rescue the NF2-related
677 schwannomatosis phenotype in vitro. Mol Ther Nucleic Acids [Internet].
678 2022;30(December):493–505. Available from:
679 https://doi.org/10.1016/j.omtn.2022.10.026

680 60. Wang Y, Xu X, Maglic D, Dill MT, Mojumdar K, Ng PKS, et al. Comprehensive Molecular
681 Characterization of the Hippo Signaling Pathway in Cancer. Cell Rep. 2018 Oct
682 30;25(5):1304-1317.e5.

683 61. James MF, Han S, Polizzano C, Plotkin SR, Manning BD, Stemmer-Rachamimov AO, et al.
684 NF2/Merlin Is a Novel Negative Regulator of mTOR Complex 1, and Activation of
685 mTORC1 Is Associated with Meningioma and Schwannoma Growth. Mol Cell Biol. 2009
686 Aug;29(15):4250–61.

687 62. Giovannini M, Bonne NX, Vitte J, Chareyre F, Tanaka K, Adams R, et al. MTORC1
688 inhibition delays growth of neurofibromatosis type 2 schwannoma. Neuro Oncol.
689 2014;16(4):493–504.

690 63. Chiasson-MacKenzie C, Vitte J, Liu CH, Wright EA, Flynn EA, Stott SL, et al. Cellular
691 mechanisms of heterogeneity in NF2-mutant schwannoma. Nat Commun [Internet].
692 2023 Mar 21;14(1):1559. Available from: https://www.nature.com/articles/s41467-
693 023-37226-0

694 64. Shi Y, Bollam SR, White SM, Laughlin SZ, Graham GT, Wadhwa M, et al. Rac1-Mediated
695 DNA Damage and Inflammation Promote Nf2 Tumorigenesis but Also Limit Cell-Cycle
696 Progression. Dev Cell. 2016 Nov 21;39(4):452–65.

697 65. Kaempchen K, Mielke K, Utermark T, Langmesser S, Hanemann CO. Upregulation of the
698 Rac1/JNK signaling pathway in primary human schwannoma cells. Hum Mol Genet.
699 2003 Jun 1;12(11):1211–21.

700 66. Lallemand D, Manent J, Couvelard A, Watilliaux A, Siena M, Chareyre F, et al. Merlin
701 regulates transmembrane receptor accumulation and signaling at the plasma
702 membrane in primary mouse Schwann cells and in human schwannomas. Oncogene.
703 2009;28(6):854–65.

704 67. Scoles DR, Nguyen VD, Qin Y, Sun CX, Morrison H, Gutmann DH, et al.
705 Neurofibromatosis 2 (NF2) tumor suppressor schwannomin and its interacting protein
706 HRS regulate STAT signaling [Internet]. Available from:
707 https://academic.oup.com/hmg/article/11/25/3179/578782

708 68. Wallesch M, Pachow D, Blücher C, Firsching R, Warnke JP, Braunsdorf WEK, et al.
709 Altered expression of E-Cadherin-related transcription factors indicates partial
710 epithelial-mesenchymal transition in aggressive meningiomas. J Neurol Sci. 2017 Sep
711 15;380:112–21.

712 69. Takahashi E, Haga A, Tanihara H. Merlin regulates epithelial-to-mesenchymal transition
713 of ARPE-19 cells via TAK1-p38MAPK-mediated activation. Invest Ophthalmol Vis Sci.
714 2015;56(4):2449–58.

715 70. Li X, Chen H, Xue L, Pang X, Zhang X, Zhu Z, et al. P53 performs an essential role in
716 mediating the oncogenic stimulus triggered by loss of expression of neurofibromatosis
717 type 2 during in vitro tumor progression. Oncol Lett. 2017;14(2):2223–31.

718 71. Beltrami S, Kim R, Gordon J. Neurofibromatosis Type 2 Protein, NF2: An uncoventional
719 cell cycle regulator.

720 72. Toshiyuki Nakayama, Yang Cheul Cho, Yuka Mine, Ayumi Yoshizaki, Shinji Naito, Chun
721 Yang Wen, et al. WJG-12-6182 (1). World J Gastroenterol. 2006;38(12):6182–7.

722

723

724 **TABLE**

Table 1. iPSCs lines information

Generation method		Reprogramming VS		Editing iPSCs from VS		Editing FiPS Ctrl 1-SV4F-7	
iPS Cell line		**VSi-25**	**VSi-267**	**VSi-25-CasD7**	**VSi-267-CasD2**	**FiPS-CasB2**	**FiPS-CasH6**
NF2 Genotype	***Allele A***	c.1736A>G	c.784C>T	c.1736A>G	c.784C>T	c.212_213delCA	c.211dup
	Allele B	WT	WT	c.211dup	c. 212_213del	WT	c.212_213del
	Protein	p.(Lys579Arg)	p.(Arg262*)	p.(Lys579Arg) & p.(Thr71Asnfs*15)	p.(Arg262*) & p.(Thr71Serfs*14)	p.(Thr71Serfs*14)	p.(Thr71Asnfs*15) & p.(Thr71Serfs*14)
	***NF2* (+/-)**		***NF2* (+/-)**	***NF2* (-/-)**	***NF2* (-/-)**	***NF2* (+/-)**	***NF2* (-/-)**
Effect		Splicing	Nonsense	Splicing and frameshift	Nonsense and frameshift	Frameshift	Frameshift
Affected exons		15	8	2 and 15	2 and 8	2	2

725

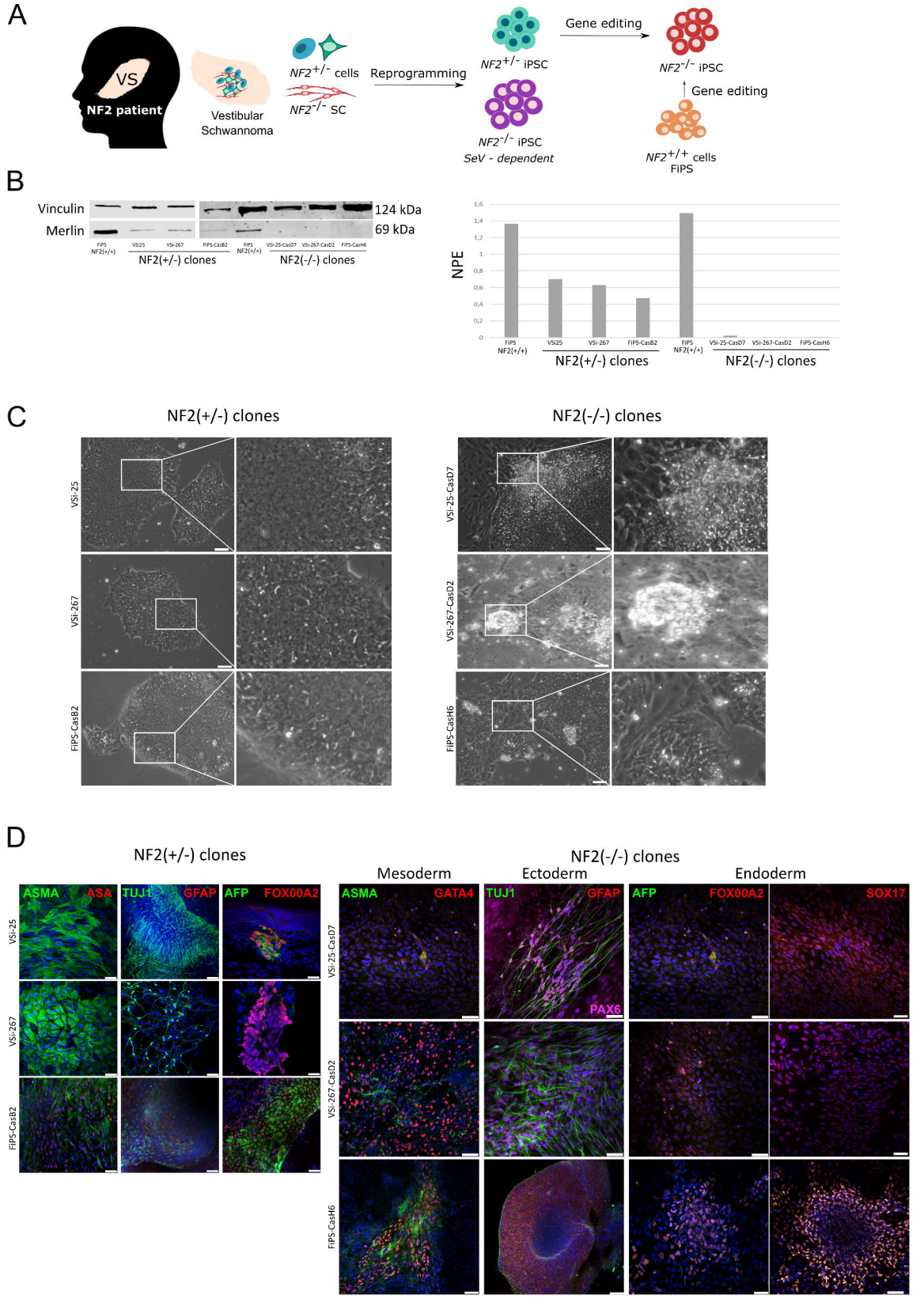
A
VS
NF2 patient
Vestibular Schwannoma
NF2+/- cells
NF2-/- SC
Reprogramming
NF2+/- iPSC
NF2-/- iPSC
SeV - dependent
Gene editing
NF2-/- iPSC
Gene editing
NF2+/+ cells
FiPS
B
Vinculin
Merlin
124 kDa
69 kDa
FiPS NF2(+/+)
VSi25
VSi-267
FiPS-CasB2
FiPS NF2(+/+)
VSi-25-CasD7
VSi-267-CasD2
FiPS-CasH6
NF2(+/-) clones
NF2(-/-) clones
NPE
1,6
1,4
1,2
1
0,8
0,6
0,4
0,2
0
NF2(+/-) clones
NF2(-/-) clones
C
NF2(+/-) clones
NF2(-/-) clones
VSi-25
VSi-267
FiPS-CasB2
VSi-25-CasD7
VSi-267-CasD2
FiPS-CasH6
D
NF2(+/-) clones
NF2(-/-) clones
Mesoderm
Ectoderm
Endoderm
ASMA
ASA
TUJ1
GFAP
AFP
FOX00A2
ASMA
GATA4
TUJ1
GFAP
PAX6
AFP
FOX00A2
SOX17
VSi-25
VSi-267
FiPS-CasB2
VSi-25-CasD7
VSi-267-CasD2
FiPS-CasH6

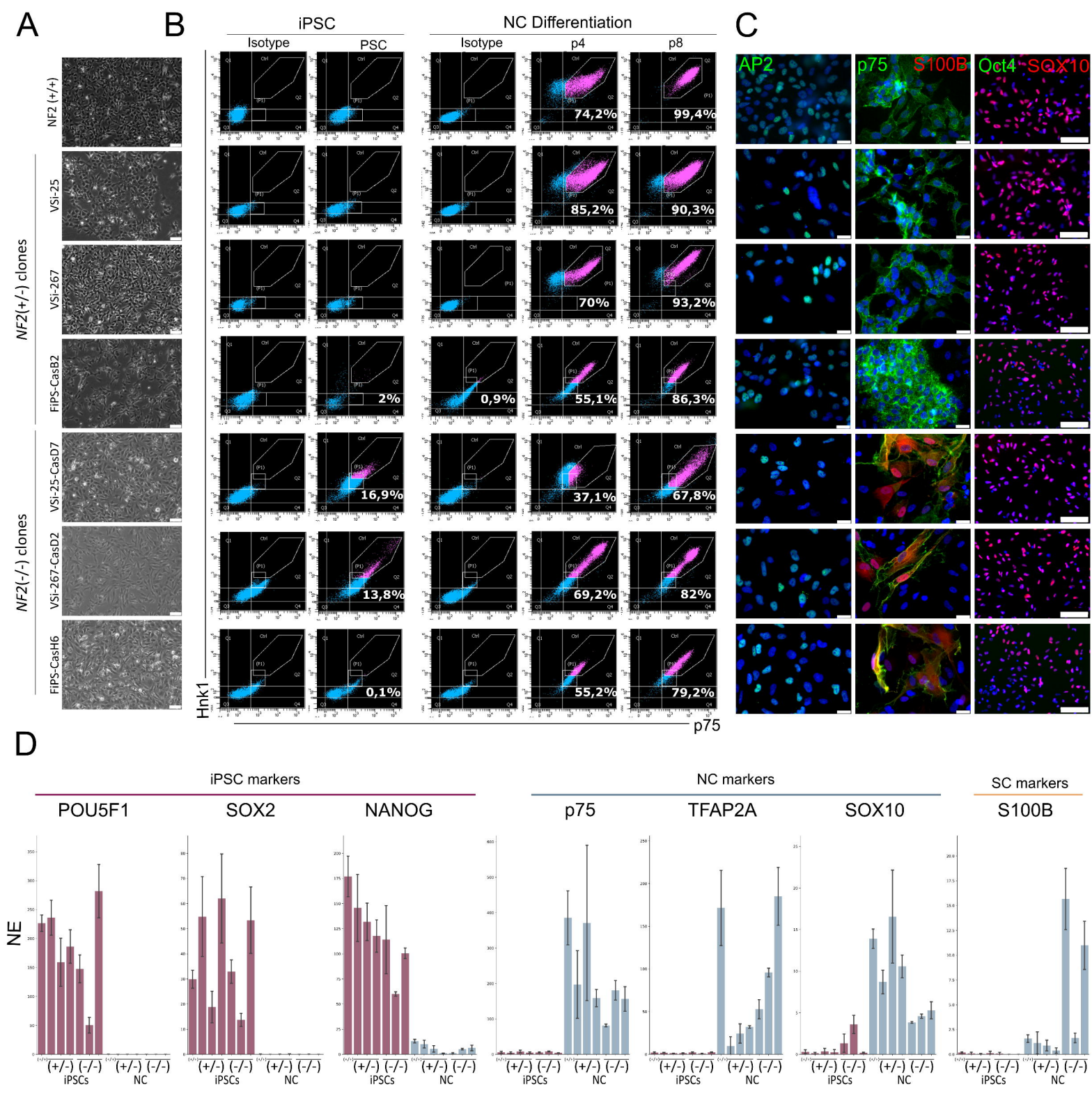
A
B
C
D
iPSC
NC Differentiation
Isotype
PSC
p4
p8
NF2 (+/+)
VSi-25
VSi-267
FiPS-CasB2
VSi-25-CasD7
VSi-267-CasD2
FiPS-CasH6
NF2(+/-) clones
NF2(-/-) clones
74,2%
99,4%
85,2%
90,3%
70%
93,2%
2%
0,9%
55,1%
86,3%
16,9%
37,1%
67,8%
13,8%
69,2%
82%
0,1%
55,2%
79,2%
Hnk1
p75
AP2
p75
S100B
Oct4
SOX10
iPSC markers
NC markers
SC markers
POU5F1
SOX2
NANOG
p75
TFAP2A
SOX10
S100B
NE
(+/-)
(-/-)
iPSCs
NC

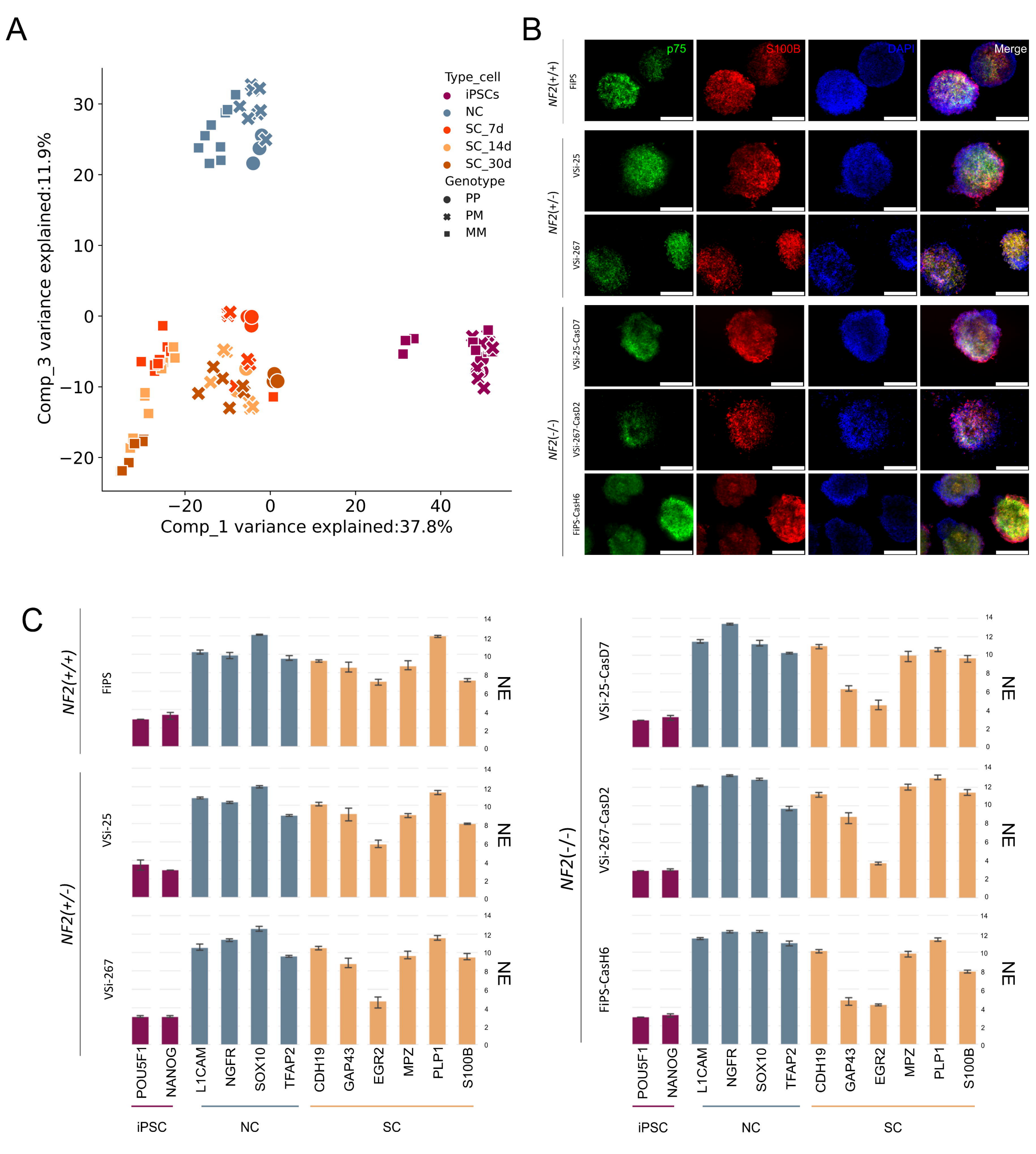
A
Type_cell
iPSCs
NC
SC_7d
SC_14d
SC_30d
Genotype
PP
PM
MM
Comp_3 variance explained:11.9%
Comp_1 variance explained:37.8%
B
p75
S100B
DAPI
Merge
NF2(+/+)
NF2(+/-)
NF2(-/-)
FiPS
VSi-25
VSi-267
VSi-25-CasD7
VSi-267-CasD2
FiPS-CasH6
C
NE
POU5F1
NANOG
L1CAM
NGFR
SOX10
TFAP2
CDH19
GAP43
EGR2
MPZ
PLP1
S100B
iPSC
NC
SC

A

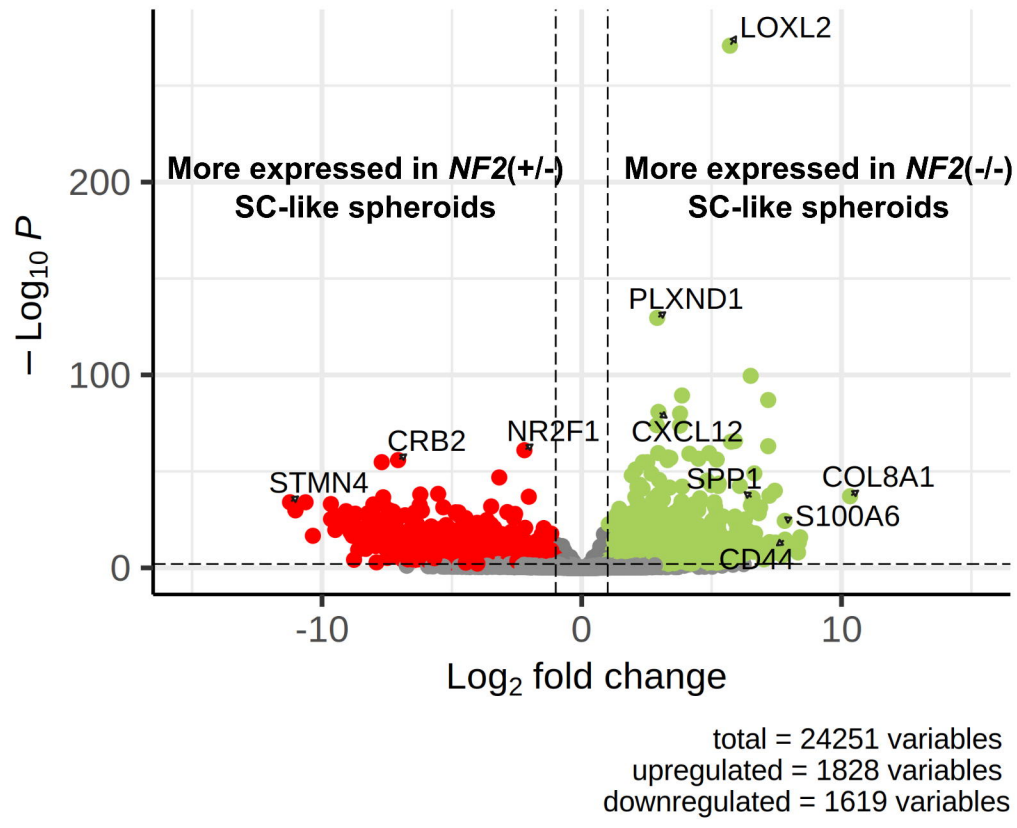
More expressed in NF2(+/-) SC-like spheroids
More expressed in NF2(-/-) SC-like spheroids
LOXL2
PLXND1
CXCL12
CRB2
NR2F1
STMN4
SPP1
COL8A1
S100A6
CD44
– Log10 P
Log2 fold change
total = 24251 variables
upregulated = 1828 variables
downregulated = 1619 variables

B

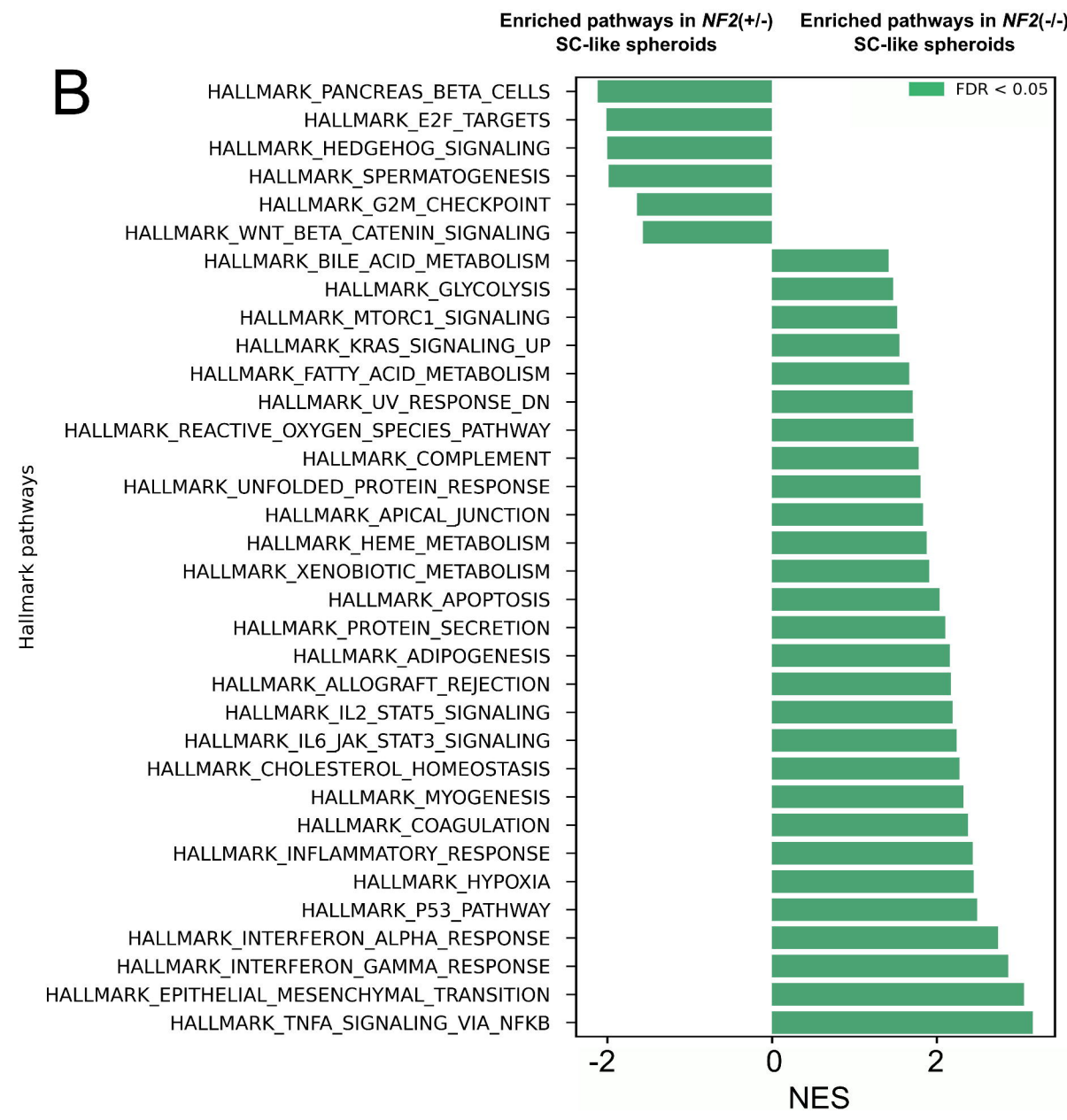
Enriched pathways in NF2(+/-) SC-like spheroids
Enriched pathways in NF2(-/-) SC-like spheroids
FDR < 0.05
HALLMARK_PANCREAS_BETA_CELLS
HALLMARK_E2F_TARGETS
HALLMARK_HEDGEHOG_SIGNALING
HALLMARK_SPERMATOGENESIS
HALLMARK_G2M_CHECKPOINT
HALLMARK_WNT_BETA_CATENIN_SIGNALING
HALLMARK_BILE_ACID_METABOLISM
HALLMARK_GLYCOLYSIS
HALLMARK_MTORC1_SIGNALING
HALLMARK_KRAS_SIGNALING_UP
HALLMARK_FATTY_ACID_METABOLISM
HALLMARK_UV_RESPONSE_DN
HALLMARK_REACTIVE_OXYGEN_SPECIES_PATHWAY
HALLMARK_COMPLEMENT
HALLMARK_UNFOLDED_PROTEIN_RESPONSE
HALLMARK_APICAL_JUNCTION
HALLMARK_HEME_METABOLISM
HALLMARK_XENOBIOTIC_METABOLISM
HALLMARK_APOPTOSIS
HALLMARK_PROTEIN_SECRETION
HALLMARK_ADIPOGENESIS
HALLMARK_ALLOGRAFT_REJECTION
HALLMARK_IL2_STAT5_SIGNALING
HALLMARK_IL6_JAK_STAT3_SIGNALING
HALLMARK_CHOLESTEROL_HOMEOSTASIS
HALLMARK_MYOGENESIS
HALLMARK_COAGULATION
HALLMARK_INFLAMMATORY_RESPONSE
HALLMARK_HYPOXIA
HALLMARK_P53_PATHWAY
HALLMARK_INTERFERON_ALPHA_RESPONSE
HALLMARK_INTERFERON_GAMMA_RESPONSE
HALLMARK_EPITHELIAL_MESENCHYMAL_TRANSITION
HALLMARK_TNFA_SIGNALING_VIA_NFKB
Hallmark pathways
NES

C

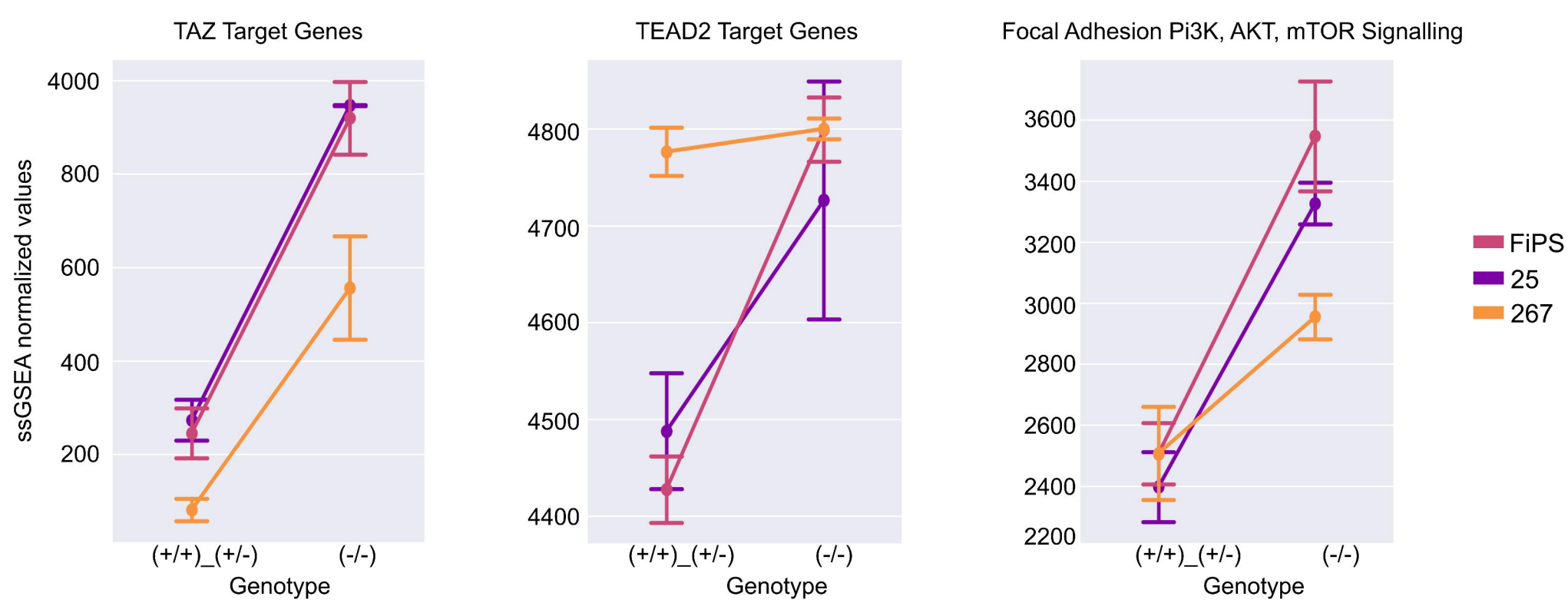
TAZ Target Genes
TEAD2 Target Genes
Focal Adhesion Pi3K, AKT, mTOR Signalling
ssGSEA normalized values
Genotype
(+/+)_(+/-)
(-/-)
FiPS
25
267

D

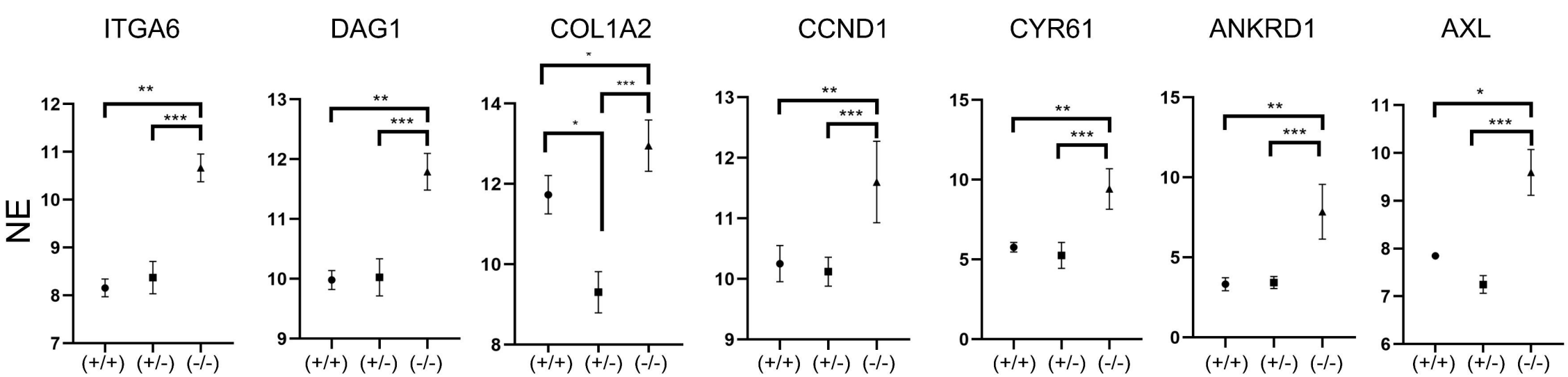
ITGA6
DAG1
COL1A2
CCND1
CYR61
ANKRD1
AXL
NE
(+/+)
(+/-)
(-/-)

A

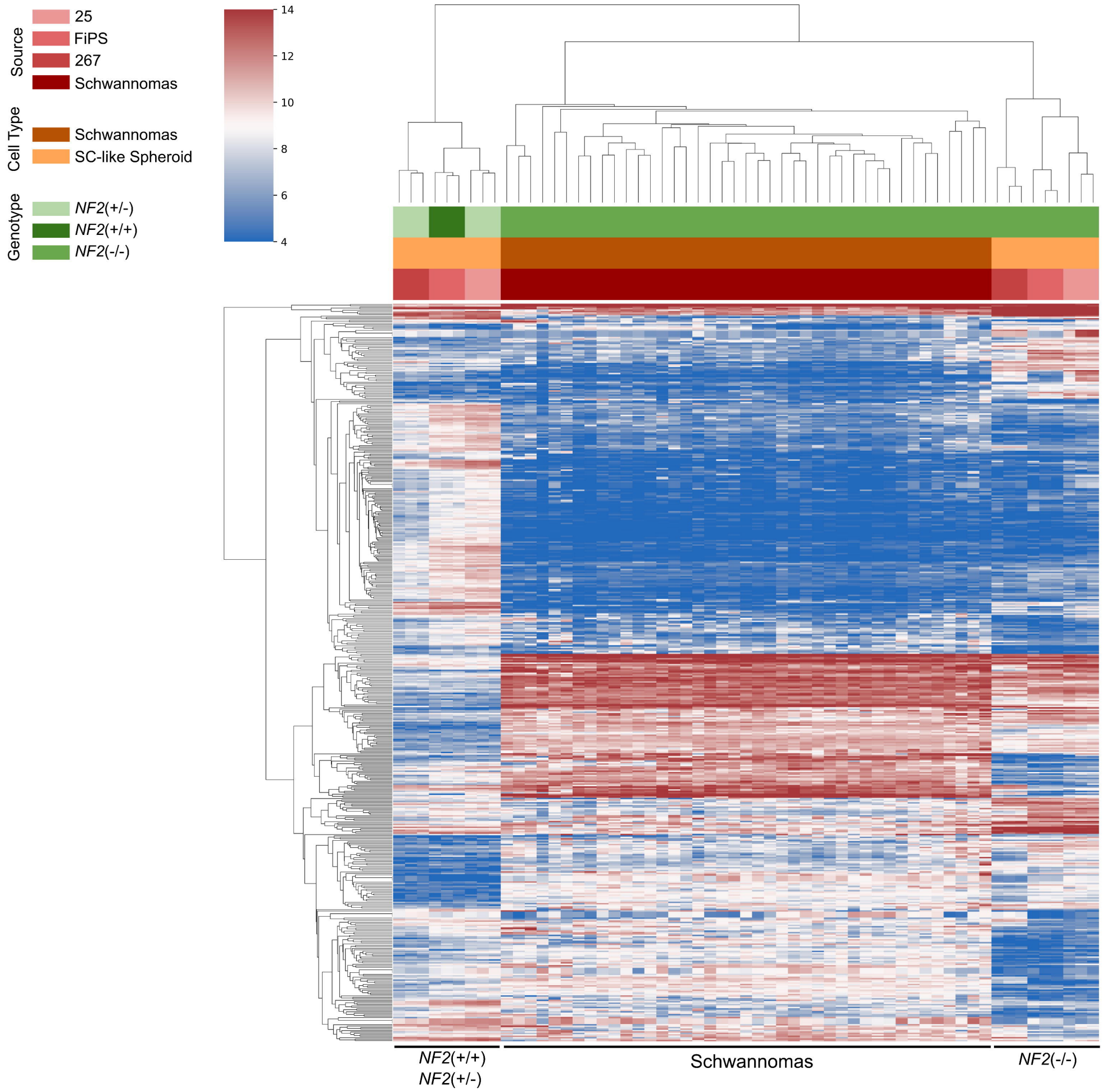
Source
25
FiPS
267
Schwannomas
Cell Type
Schwannomas
SC-like Spheroid
Genotype
NF2(+/-)
NF2(+/+)
NF2(-/-)
14
12
10
8
6
4
NF2(+/+)
NF2(+/-)
Schwannomas
NF2(-/-)

B

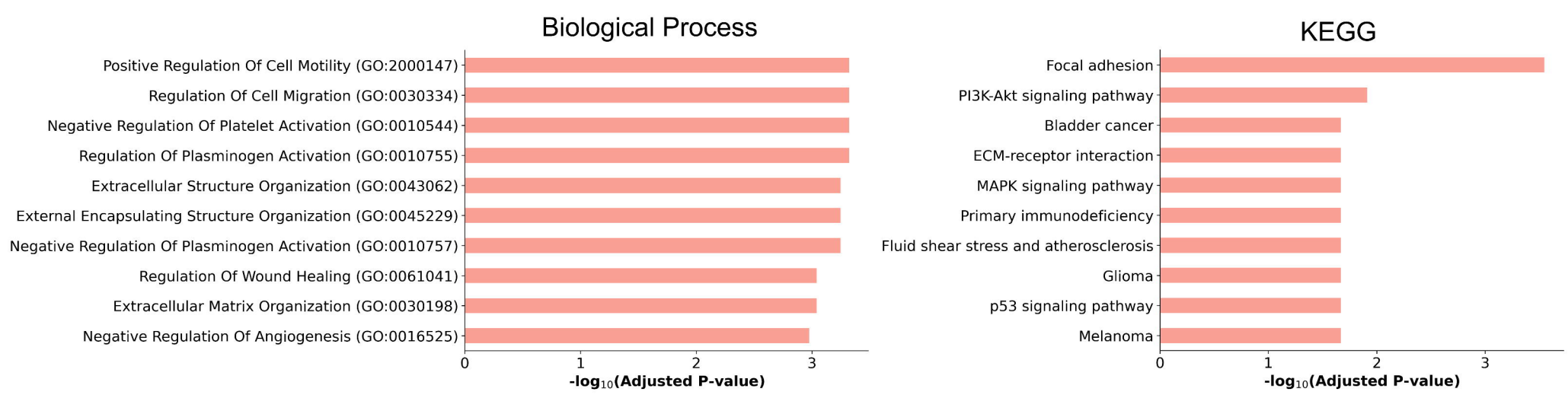
Biological Process
Positive Regulation Of Cell Motility (GO:2000147)
Regulation Of Cell Migration (GO:0030334)
Negative Regulation Of Platelet Activation (GO:0010544)
Regulation Of Plasminogen Activation (GO:0010755)
Extracellular Structure Organization (GO:0043062)
External Encapsulating Structure Organization (GO:0045229)
Negative Regulation Of Plasminogen Activation (GO:0010757)
Regulation Of Wound Healing (GO:0061041)
Extracellular Matrix Organization (GO:0030198)
Negative Regulation Of Angiogenesis (GO:0016525)
0
1
2
3
-log10(Adjusted P-value)
KEGG
Focal adhesion
PI3K-Akt signaling pathway
Bladder cancer
ECM-receptor interaction
MAPK signaling pathway
Primary immunodeficiency
Fluid shear stress and atherosclerosis
Glioma
p53 signaling pathway
Melanoma
0
1
2
3
-log10(Adjusted P-value)

C

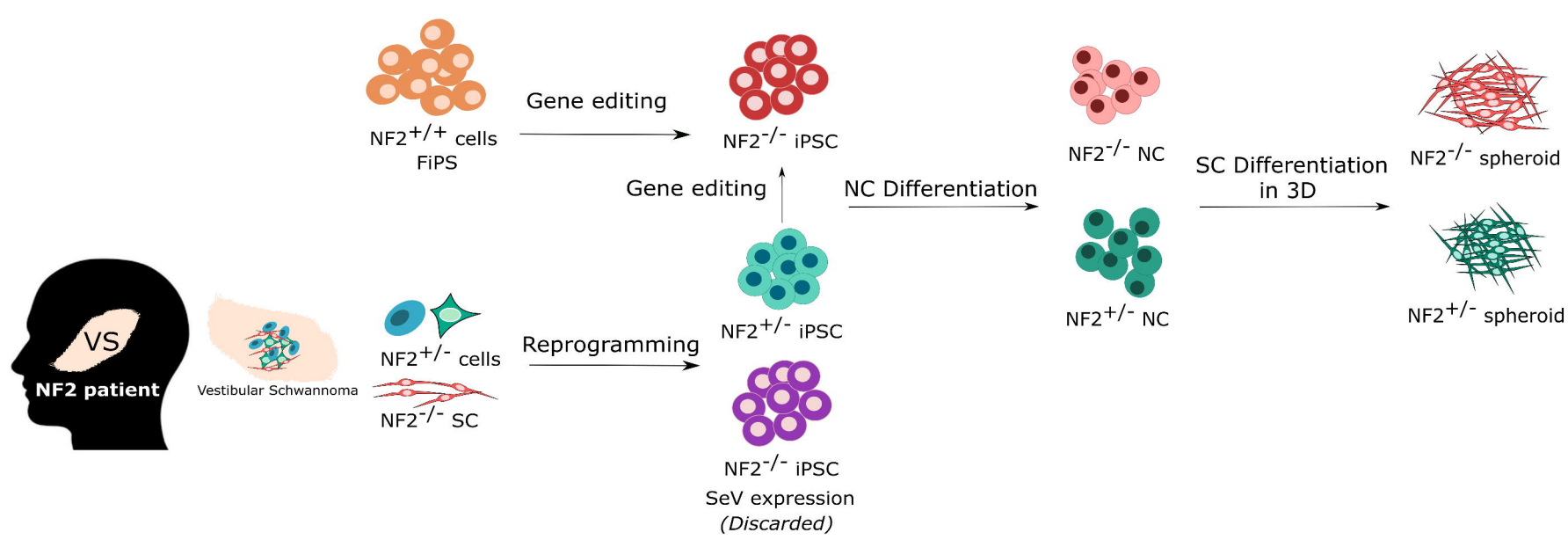
NF2+/+ cells
FiPS
Gene editing
NF2-/- iPSC
Gene editing
NC Differentiation
NF2-/- NC
SC Differentiation in 3D
NF2-/- spheroid
NF2+/- NC
NF2+/- spheroid
VS
NF2 patient
Vestibular Schwannoma
NF2+/- cells
NF2-/- SC
Reprogramming
NF2+/- iPSC
NF2-/- iPSC
SeV expression
(Discarded)